Journal of Magnetic Resonance **143,** 266–273 (2000)
doi:10.1006/jmre.1999.1990, available online at http://www.idealibrary.com on IDEAL®

Separation of Quadrupolar and Magnetic Contributions to Spin–Lattice Relaxation in the Case of a Single Isotope

A. Suter, M. Mali, J. Roos, and D. Brinkmann

Physik-Institut, Universität Zürich, CH-8057 Zürich, Switzerland

E-mail: suter@lanl.gov

Received May 17, 1999; revised October 21, 1999

We present a NMR pulse double-irradiation method which allows one to separate magnetic from quadrupolar contributions in the spin–lattice relaxation. The pulse sequence fully saturates one transition while another is observed. In the presence of a $|\Delta m| = 2$ quadrupolar contribution, the intensity of the observed line is altered compared to a standard spin-echo experiment. We calculated analytically this intensity change for spins $I = 1, \frac{3}{2}, \frac{5}{2}$, thus providing a quantitative analysis of the experimental results. Since the pulse sequence we used takes care of the absorbed radiofrequency power, no problems due to heating arise. The method is especially suited when only *one* NMR sensitive isotope is available. Different cross-checks were performed to prove the reliability of the results obtained. The applicability of this method is demonstrated by a study of the plane oxygen ^{17}O ($I = \frac{5}{2}$) in the high-temperature superconductor $YBa_2Cu_4O_8$: the ^{17}O spin–lattice relaxation rate consists of magnetic as well as quadrupolar contributions.

Key Words: **NMR; NQR; double-irradiation method; spin–lattice relaxation; quadrupolar relaxation.**

1. INTRODUCTION

The work presented in this paper has been motivated by the experience in condensed matter nuclear magnetic resonance (NMR) experiments that quite often both magnetic and quadrupolar time-dependent interactions are present, causing spin–lattice relaxation. The question arises whether it is possible to deduce, directly from the experiment, the admixture of the two different contributions to the overall relaxation.

The literature contains mainly calculations of multiexponential magnetization recovery laws for the case of either *purely* magnetic or *purely* quadrupolar fluctuations, with Andrew and Tunstall (*1*) being the first to treat the case of a static quadrupolar perturbed Zeeman Hamiltonian (spin $I = \frac{3}{2}, \frac{5}{2}$). These calculations were extended to higher spins (*2–5*) and to the case of a static quadrupolar Hamiltonian (*6–9*). MacLaughlin *et al.* (*10*) treated the case of a static quadrupolar Hamiltonian ($\eta = 0$) with mixed fluctuations in a kind of perturbation expansion, whereas Rega (*11*) presented, for this case, an exact solution in the limit of time approaching zero.

In a previous study (*12*), we discussed the multiexponential recovery for the case of a static quadrupolar perturbed Zeeman Hamiltonian in the presence of both magnetic and quadrupolar fluctuations under the assumption that the spin-exchange coupling can be omitted and the eigenfunctions of the static Hamiltonian can be approximated by Zeeman eigenfunctions. We found that, in a surprisingly large region of the parameter space spread by the probabilities for magnetic and quadrupolar induced transitions, it is almost impossible, within experimental errors, to separate magnetic and quadrupolar contributions to the relaxation. Instead, the "dominant" contribution determines the time evolution of the recovery law; i.e., the system can approximately be described by a *single* time constant, T_1^{eff}. However, it is questionable whether this approximation is meaningful in the presence of mixed relaxation or whether it is more appropriate to describe the system by the *separate* transition probabilities.

If the nucleus under consideration has *two* magnetic isotopes as in the case of copper (^{63}Cu and ^{65}Cu), the admixture can be estimated from the ratio of the relaxation times, T_1. Nevertheless, the precision needed for a reliable interpretation of this ratio is commonly underestimated.

In this publication we will present a method, which enables the experimentalist to separate the different contributions of the spin–lattice relaxation especially in the case where the element under consideration has only *one* NMR sensitive isotope. The method involves a special initial condition of the spin system which we call dynamic saturation and which had already been mentioned briefly in our previous work (*12*). The method presented here is an extension of the pioneering work of Pound (*13*).

The paper is organized as follows. The next section will introduce the theoretical background essential to understand the method. In Section 3 we will give the results including a discussion, and Section 4 will show experimental results of ^{17}O NMR in $YBa_2Cu_4O_8$, including a more technical discussion of the experiment.

1090-7807/00 $35.00

2. BASIC RELATIONS AND MASTER EQUATION

For simplicity and the reader's convenience, we repeat part of our treatment presented in Ref. (*12*). The starting point is the Hamiltonian

$$\mathcal{H}_{\text{tot}} = \mathcal{H}_0 + \mathcal{H}_1(t),$$

where $\mathcal{H}_0 = \mathcal{H}_Z + \mathcal{H}_Q$ describes the time-independent (or "static") Hamiltonian which comprises the Zeeman interaction, $\mathcal{H}_Z$, with the external magnetic field and the quadrupolar interaction, $\mathcal{H}_Q$, with the internal electric field gradient (EFG) tensor. $\mathcal{H}_1(t)$ takes into account fluctuations; it is the sum of a magnetic and a quadrupolar contribution,

$$\mathcal{H}_1(t) = \mathcal{H}_{\text{mag}}(t) + \mathcal{H}_{\text{quad}}(t), \qquad [1]$$

where

$$\mathcal{H}_{\text{mag}}(t) = -\hbar\gamma_n \mathbf{I}\cdot\mathbf{h}(t)$$

$$\mathcal{H}_{\text{quad}}(t) = \frac{eQ}{4I(2I-1)}\sum_{k=-2}^{2} V_k(t)T_{2k}(\mathbf{I}).$$

Here, $\mathbf{I}$ is the nuclear spin operator, $\mathbf{h}(t)$ is a fluctuating magnetic field, $V_k(t)$ is a component of the fluctuating EFG, and $T_{2k}(\mathbf{I})$ are spherical tensor operators (*14, 15*).

In Eq. [1], nuclear spin-exchange terms were omitted. If the quadrupolar splitting, due to $\mathcal{H}_Q$, is large compared to the nuclear spin-exchange coupling, the time evolution of the spin–lattice relaxation proceeds by the direct coupling to the lattice. Cases where the nuclear spin-exchange terms are important are discussed in Refs. (*1, 16*).

The relaxation of the spin system toward its thermodynamic equilibrium is described by the so-called master equation

$$\frac{d}{dt}\mathbf{P}(t) = \mathbf{W}\{\mathbf{P}(t) - \mathbf{P}(0)\}. \qquad [2]$$

Here, $\mathbf{P}(t)$ is the population vector of the different energy levels with $\mathbf{P}(0)$ being the equilibrium value. The relaxation matrix, $\mathbf{W}$, is, in second-order perturbation theory, given by (*14*)

$$W_{\alpha\beta} \overset{\alpha\neq\beta}{=} \frac{1}{\hbar^2}\int_{-\infty}^{\infty} d\tau\, \exp(i\omega_{\alpha\beta}\tau)\overline{\langle\alpha|\mathcal{H}_1(\tau)|\beta\rangle\langle\beta|\mathcal{H}_1(0)|\alpha\rangle}$$

$$W_{\alpha\alpha} = -\sum_{\beta\neq\alpha} W_{\alpha\beta},$$

where $|\alpha\rangle$, $|\beta\rangle$ are eigenstates of $\mathcal{H}_0$ and $\omega_{\alpha\beta} = (\langle\alpha|\mathcal{H}_0|\alpha\rangle - \langle\beta|\mathcal{H}_0|\beta\rangle)/\hbar$ are transition frequencies. Ensemble averages are denoted by $\overline{\langle\ldots\rangle}$.

As long as the eigenfunctions of $\mathcal{H}_0$ can be approximated by the eigenfunctions of a Zeeman Hamiltonian, i.e., $\|\mathcal{H}_Z\| \gg \|\mathcal{H}_Q\|$, the relevant relaxation matrix terms for magnetic and quadrupolar relaxation are given as

$$W_{\alpha\beta}^{\text{mag}} = J(\omega_{\alpha\beta})\cdot\{|\langle\alpha|I^+|\beta\rangle|^2 + |\langle\alpha|I^-|\beta\rangle|^2\}$$

$$W_{\alpha\beta}^{\text{quad,1}} = J^{(1)}(\omega_{\alpha\beta})\cdot\{|\langle\alpha|I^+I_z + I_zI^+|\beta\rangle|^2 + |\langle\alpha|I^-I_z + I_zI^-|\beta\rangle|^2\}$$

$$W_{\alpha\beta}^{\text{quad,2}} = J^{(2)}(\omega_{\alpha\beta})\cdot\{|\langle\alpha|(I^+)^2|\beta\rangle|^2 + |\langle\alpha|(I^-)^2|\beta\rangle|^2\}.$$

The J's are the spectral densities of the fluctuating fields,

$$J(\omega) = \frac{\gamma_n^2}{2}\int_{-\infty}^{\infty} d\tau\, \exp(i\omega\tau)[h_+,\, h_-]$$

$$J^{(1,2)}(\omega) = \left(\frac{eQ}{\hbar}\right)^2\int_{-\infty}^{\infty} d\tau\, \exp(i\omega\tau)[V_{+1,2},\, V_{-1,2}]$$

with $[A, B] = (\frac{1}{2})\overline{(A(\tau)B(0) + B(\tau)A(0))}$, $h_\pm = h_x \pm ih_y$, $V_{\pm1} = V_{xz} \pm iV_{yz}$, and $V_{\pm2} = \frac{1}{2}(V_{xx} - V_{yy}) \pm iV_{xy}$.

If $\mathcal{H}_Z$ and $\mathcal{H}_Q$ are of similar magnitude, the situation is more complicated. The case of *purely magnetic fluctuations*, for $\|\mathcal{H}_Z\| \approx \|\mathcal{H}_Q\|$, has been treated by various authors (*17, 18*).

In this paper, we will deal with the case $\|\mathcal{H}_Z\| \gg \|\mathcal{H}_Q\|$ and we make the additional assumption that the spectral densities can be approximated by a single value. This means that the inverse of the correlation time, τ_c^{-1}, of the fluctuating fields is large compared to $\omega_{\alpha\beta}$, that is, $\omega_{\alpha\beta}\tau_c \ll 1$. One then obtains

$$J(\omega) \simeq J(0) =: W$$

$$J^{(1,2)}(\omega) \simeq J^{(1,2)}(0) =: W_{1,2}$$

and the resulting transition probabilities become

$$W_{m\to m-1}^{\text{mag}} = W(I+m)(I-m+1)$$

$$W_{m\to m-1}^{\text{quad,1}} = W_1\frac{(2m-1)^2(I-m+1)(I+m)}{2I(2I-1)^2}$$

$$W_{m\to m-2}^{\text{quad,2}} = W_2\frac{(I+m)(I+m-1)\times(I-m+1)(I-m+2)}{2I(2I-1)^2}.$$

Our calculations were performed in the high-temperature limit, i.e., $\hbar\omega_{\alpha\beta} \ll k_BT$, so that a further simplification takes place: $W_{\alpha\to\beta} \simeq W_{\beta\to\alpha}$. Figure 1 sketches the various transition probabilities which are possible for a $\frac{5}{2}$ spin system. We assume the

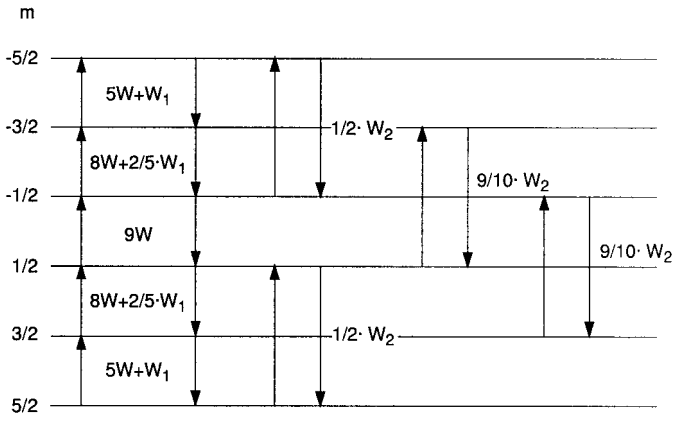

FIG. 1. Transitions between the spin energy levels effected by magnetic and quadrupolar spin–lattice relaxation processes for $I = \frac{5}{2}$.

spacings between the levels to be sufficiently unequal to suppress spin-exchange transitions.

To solve the master equation, Eq. [2], it is convenient to introduce some abbreviations. The population of level m is P_m and we define the difference in population between adjacent levels by $P_{m+1/2} = P_{m+1} - P_m$; the equilibrium value of this difference is $n_0 = P_{m+1}(0) - P_m(0)$. The deviation of the population difference from its equilibrium value is denoted by $N_{m+1/2} = P_{m+1/2} - n_0$; the values $N_{m+1/2}$ form the vector $\mathbf{N}$.

Given the transition probabilities as shown in Fig. 1, we can write down, in compact form, the following "reduced" master equation for $\mathbf{N}$,

$$\frac{d}{dt}\mathbf{N} = \mathbf{R}\mathbf{N}, \qquad [3]$$

where $\mathbf{R}$ is the reduced relaxation coefficient matrix. The solution of Eq. [3] is of the form

$$N_j(t) = \sum_i [(\mathbf{E}^{\mathrm{T}})^{-1}\mathbf{N}(0)]_i E_{ij} \exp(t\lambda_i), \qquad [4]$$

where λ_i and $\mathbf{E}$ are the eigenvalues and the eigenvector matrix of $\mathbf{R}$, respectively, and $\mathbf{E}^{\mathrm{T}}$ denotes the transpose of $\mathbf{E}$. $\mathbf{N}(0)$ is the vector describing the initial condition of the spin system into which it has been brought during a certain preparation period.

Once the $N_j(t)$ are known, the corresponding time-dependent magnetization, $M(t)$, is obtained,

$$M(t) = M(\infty)[1 - \sum_i a_i \exp(t\lambda_i)] \qquad [5]$$

and the a_i are given by

$$a_i = -\frac{1}{n_0}[(\mathbf{E}^{\mathrm{T}})^{-1}\mathbf{N}(0)]_j E_{ji}, \qquad [6]$$

where the index j refers to the line which will be observed, e.g., the central transition. Usually, the irradiated line and the observed line are the same.

We will now consider an experiment, which we call *dynamic saturation*, with a special initial condition; this pulse sequence will allow us to disentangle quadrupolar from magnetic contributions in the spin–lattice relaxation. We saturate a selected line, q, for instance, by a long comb of pulses in such a way that the comb length, T_{tot}, is much larger than $1/\min(W, W_1, W_2)$ and that the pulse spacing, T_{CD}, within the comb satisfies the condition $5T_2 < T_{CD} \ll 1/\max(W, W_1, W_2)$. This situation contrasts with an adiabatic manipulation of the spin system where, with the spin system initially in equilibrium, a short radiofrequency (RF) pulse is applied to one of the transitions. In the case of dynamic saturation, the initial condition must be calculated since the stimulating RF field causes transitions, with transition rate P_{RF}, between the levels $q + \frac{1}{2}$ and $q - \frac{1}{2}$. Thus, for calculating the initial condition vector, the rate Eq. [3] must be extended in the following way:

$$\frac{d}{dt}\mathbf{N} = (\mathbf{R} + \mathbf{S})\mathbf{N} + n_0\mathbf{P}.$$

$\mathbf{S}$ is a square matrix with all elements zero except $S_{q\pm1,q} = P_{\mathrm{RF}}$, $S_{q,q} = -2P_{\mathrm{RF}}$. $\mathbf{P}$ is a vector with all the elements zero except $P_{q\pm1} = P_{\mathrm{RF}}$, $P_q = -2P_{\mathrm{RF}}$. For dynamic equilibrium, when $d\mathbf{N}/dt = 0$, we have

$$\mathbf{N}(\infty) = -n_0(\mathbf{R} + \mathbf{S})^{-1}\mathbf{P}.$$

$\mathbf{N}(\infty)$, which becomes the initial condition vector $\mathbf{N}(0)$ for solving Eq. [3], is calculated under the assumption that $P_{\mathrm{RF}} \gg \max(W, W_1, W_2)$. The exact formulas for $\mathbf{N}(0)/n_0$ are given in the Appendix.

3. TRANSITION ENHANCEMENT BY DYNAMIC SATURATION

Let us deal, for the moment, with the special situation of *pure* magnetic relaxation, i.e., $W_1, W_2 = 0$. In this case, after dynamic saturation, the $\mathbf{N}(0)$'s for all spin values $I \geq 1$ take the form

$$\mathbf{N}(0)/n_0 = [0, \ldots, 0, -1, 0, \ldots, 0],$$

where -1 refers to the irradiated line. This equation reflects the following behavior. On the timescale of the spin–lattice relaxation, $T_1 = 1/(2W)$, the new population differences are the

same as in the case of thermodynamic equilibrium, except for the irradiated line. That means that a spectrum obtained by adiabatic manipulation (e.g., in a standard spin-echo experiment) is identical to the corresponding spectrum due to dynamic saturation, except for the irradiated line. This is not true anymore in the case of mixed or pure quadrupolar relaxation as we will show now.

The intensity of a specific transition which we observe will be denoted as follows. For the transition $m \rightarrow m - 1$, I_{ad}^{m} is measured by an adiabatic pulse sequence as in the case of a standard $\pi/2 - \pi$ spin-echo experiment; $I_{\mathrm{dyn}}^{m,n}$ refers to the same transition, however, in the presence of dynamic saturation of the transition $n \rightarrow n - 1$. Given this notation, we define an *enhancement factor* by

$$E_m^n = \frac{I_{\mathrm{dyn}}^{m,n}}{I_{\mathrm{ad}}^{m}} = 1 + \left(\frac{\mathbf{N}(0)}{n_0}\right)_{m-1/2}.$$

With the results of the Appendix we get, for instance, for a spin $I = \frac{5}{2}$ system with the central transition being dynamically saturated and the inner satellite being observed,

$$\begin{aligned} E_{\mathrm{inner}}^{\mathrm{central}} &= 1 + \mu_5/\zeta_1 \\ \mu_5 &= 45W_2(10W + 2W_1 + W_2) \\ \zeta_1 &= 4000W^2 + 1000WW_1 + 40W_1^2 + 1100WW_2 \\ &\quad + 160W_1W_2 + 45W_2^2. \end{aligned}$$

The enhancement factor is *one* in the case of pure magnetic relaxation but it is nontrivial in the case of mixed or pure quadrupolar relaxation.

That the enhancement factor is a nontrivial function of the relaxation process was already noticed by Pound (*13*), who used it to show that the relaxation of ^{23}Na($I = \frac{3}{2}$, 100% abundance) in $NaNO_3$ is purely quadrupolar.

Figure 2 shows, for a spin $I = \frac{5}{2}$ system with mixed relaxation, contour plots of the enhancement factor as a function of W_1/W and W_2/W. Similar results, however less pronounced, are found for other combinations of $n \rightarrow n - 1$ and $m \rightarrow m - 1$.

The characteristic results are as follows. (i) The enhancement effect is less pronounced in the case of mixed relaxation as compared to pure quadrupolar relaxation. This makes it more difficult to detect the effect, although not impossible because of the very high time stability of modern spectrometers. (ii) There is always at least one transition with an appreciable enhancement factor [e.g., the cases (a) and (c) in Fig. 2], whereas the other transitions are "depressed" [cases (b) and (d)]. This feature can be used for cross-checking the experiment if one is able to observe both transitions at the same time; this will be demonstrated in the next section. (iii) The enhancement factor depends only weakly on W_1/W since W_1 connects,

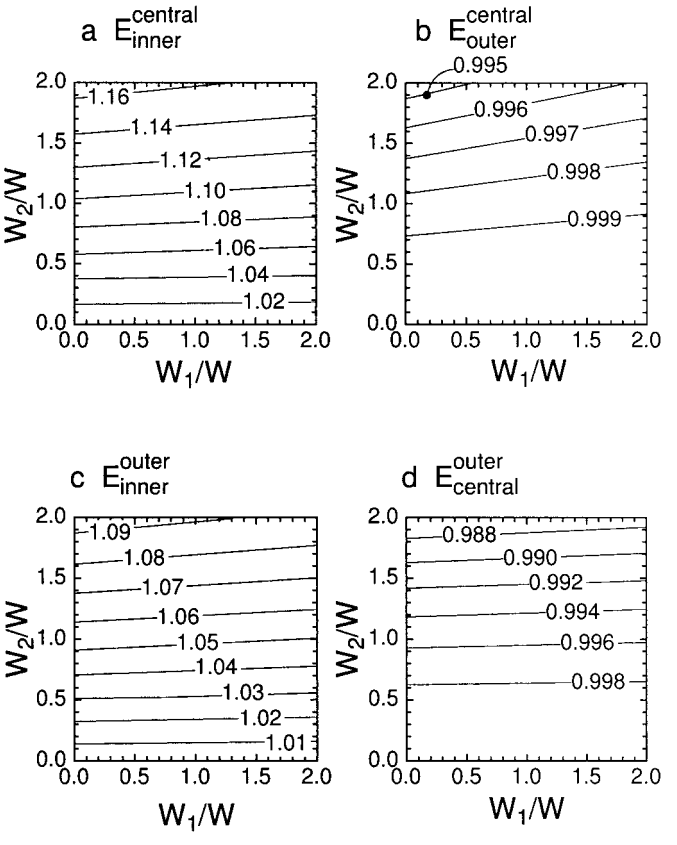

FIG. 2. Contour plots of the enhancement for a spin $I = \frac{5}{2}$ system in the case of mixed relaxation. (a) and (b) correspond to saturation of the central transition, and (c) and (d) to saturation of the outer satellite.

except for the $(-\frac{1}{2}, \frac{1}{2})$ transition, the same levels as W does, which has no effect on the enhancement function. Therefore, measuring the enhancement yields information only about the quadrupolar $\Delta m = 2$ transitions.

4. EXPERIMENTAL DETAILS

We will discuss experimental details guided by our study of the high-temperature superconductor $YBa_2Cu_4O_8$; these investigations will be published elsewhere (*19*).

The experiment was performed by using a combination of two standard pulse spectrometers together with a magnetic field of $B_0 = 8.9945$ T ($B_0 \| c$). The resonant circuit was damped by a 12-Ω resistor in order to achieve a broad frequency range. The resonance signals were obtained by a phase alternating add–subtract spin-echo technique similar to that described in Ref. (*20*) followed by Fourier transformation of the spin echo.

Each experiment consists of a certain combination of pulse sequences which are shown in Fig. 3. To measure I_{dyn}, we apply the *saturation* and the *detection* sequence. In the first sequence, dynamic saturation of the $n \rightarrow n - 1$ transition is achieved by applying pulses C and D. The spacing between

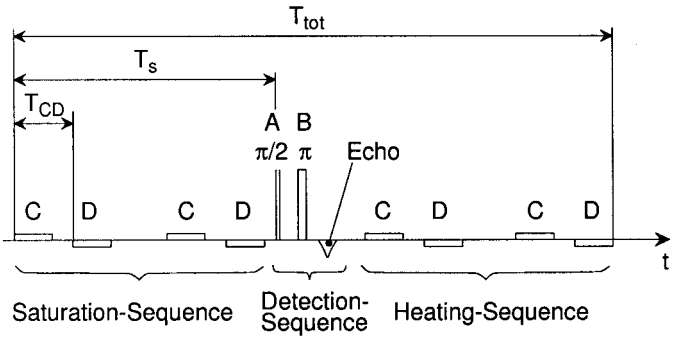

FIG. 3. Pulse sequence used in the experiment. Details are described in the text.

these pulses, T_{CD}, has to be much larger than T_2 and much shorter than T_1; i.e., $5T_2 < T_{CD} \ll T_1$ ($T_{CD} = 1.5$ ms in our experiment). The length of these pulses is chosen very large (20 μs) in order to saturate the $n \rightarrow n - 1$ transition only. Furthermore, we change the phase between the *C* and *D* pulses by 90° to get rid of possible coherence effects. The total length of the saturation sequence, T_s, has to be of the order of the longest effective relaxation time. The *detection* sequence is the usual spin-echo $\pi/2$–π pulse sequence. Here, we use very intense pulses (the $\pi/2$ pulse length is about 1 μs) to observe both the central transition and the high-frequency satellites in a single shot.

In order to measure I_{ad}, we apply, of course, the detection sequence, but it must be supplemented by a *heating* sequence. Since pulsing heats the sample, a comparison of line intensities of different experiments (standard spin echo and dynamic saturation) requires constant sample temperature. This is achieved by making the heating and the saturation sequence identical so that the total power absorbed by the sample is the same in either case. In other words, the total length of the pulse sequence, T_{tot}, is kept fixed ($T_{tot} = 400$ ms in our case). From our previous experiments on the isotope effect of the spin gap (*22*) we know that, at about 95 K, a constant temperature is achieved after running the heating sequence for about 5 min. A combination of all three pulse sequences is used to cross-check our results; this will be discussed further below.

To illustrate the method, we present ^{17}O spectra from $YBa_2Cu_4O_8$ taken at $T = 95$ K; see Fig. 4. This superconductor contains, beside the apex oxygen, plane oxygen sites, O(2) and O(3), in the CuO_2 plane, where superconductivity takes place, and a chain oxygen site, O(1). Since the magnetic shifts of the different sites are very small in this compound (*21*), the central transitions of all sites coincide. Here, we are only interested in the plane sites. Figure 4, top (a), shows the ^{17}O spectrum as obtained by Fourier transform of the standard echo. All central transitions coincide and all O(1) satellites nearly coincide, while inner and outer O(2, 3) satellites are well separated. The splitting of these satellites is due to the orthorhombic symmetry ($a = 3.8411$ Å, $b = 3.8718$ Å) of the crystal.

Figure 4, top (b), presents the ^{17}O spectrum after dynamic saturation of the central transition and Fig. 4, top (c), gives the difference between the "saturation" and the "standard." Because of the short *A* and *B* pulses, all transitions can be observed. Obviously, the central transition is saturated; note the "negative" intensity. Whereas the central transition of the plane oxygen is totally saturated, the central transition as well

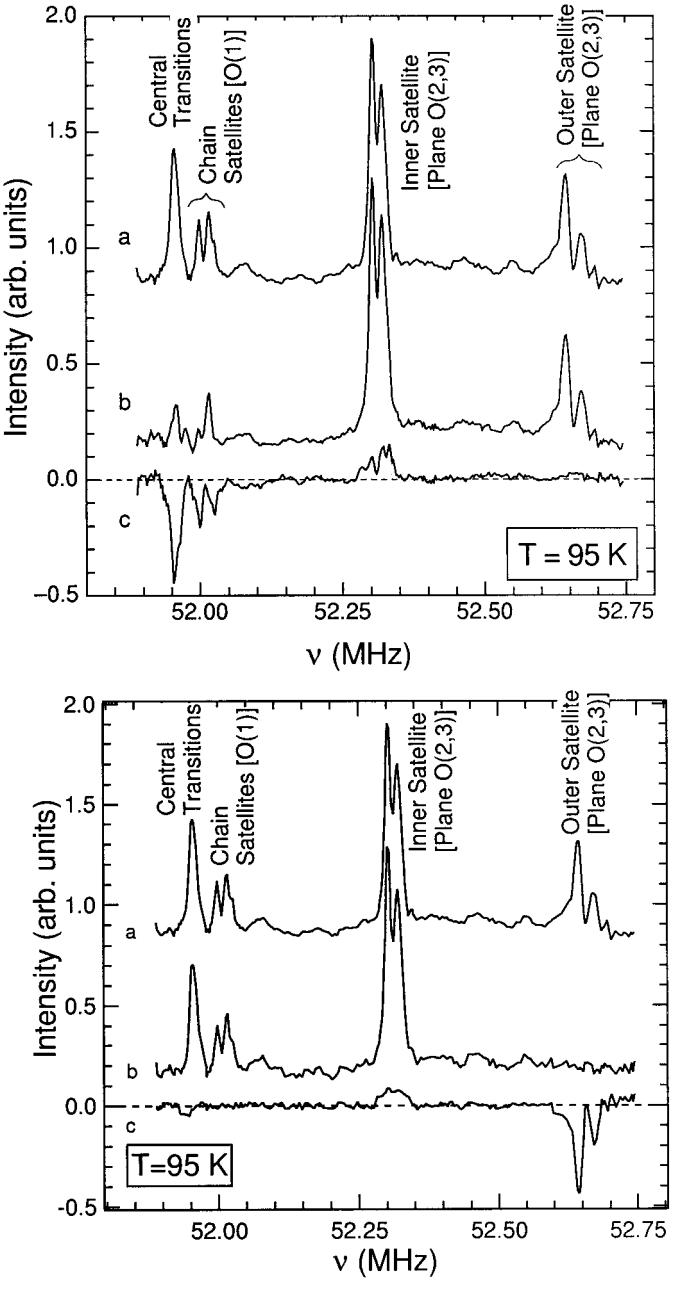

FIG. 4. Top: (a) ^{17}O central transitions and high-frequency satellites of plane oxygen, O(2) and O(3), and chain oxygen sites, O(1), in $YBa_2Cu_4O_8$. (b) Spectrum obtained after dynamic saturation of the central transition. (c) Difference of (b) and (a) spectrum. Bottom: Analogous to top panel, but with dynamic saturation of the outer satellite.

as the satellites of chain oxygen is not. This is due to the fact that the chain oxygen nuclei have a considerably shorter T_1 than the plane nuclei and that the pulse sequence was optimized for plane oxygen. That this is actually true can be seen from Fig. 4 bottom, which shows the symmetric experiment where we dynamically saturated the outer high-frequency satellite.

The most important feature is the remaining *positive* intensity of the difference spectrum at the position of the inner high-frequency satellite. According to the discussion above and, in particular, the contour plot of Fig. 2a, this intensity enhancement clearly shows that there is a quadrupolar contribution to the relaxation of the plane oxygen nuclei. This conclusion is supported by the fact that the intensity at the position of the *outer* high-frequency satellite is almost zero [see Fig. 4 top (c)] in agreement with the contour plot of Fig. 2b.

The amount of quadrupolar admixture to the overall spin–lattice relaxation is determined as follows. Experimentally, the intensity enhancement of the inner satellite (when the central transition is dynamically saturated) is 1.13(2) which then results in a ratio $W_2/W = 1.4(3)$ according to Fig. 2a. If we saturate the *outer* high-frequency satellite, the intensity enhancement of the inner satellite is 1.04(2), leading to a ratio of $W_2/W = 0.7(4)$ according to Fig. 2c. The weighted average is $W_2/W = 1.15(25)$.

Even though the values of W_2/W overlap within the estimated errors, it is worthwhile to ask whether their discrepancy is of physical origin. As stated in Section 2, we explicitly excluded spin-exchange coupling when deriving the enhancement factor. However, if present, this coupling could lead to the observed difference. If the central transitions, which coincide for all different oxygen sites (as mentioned above), are saturated, then flip-flop transitions between oxygen at different sites will be suppressed and, since the quadrupolar coupling differs from site to site, there is *negligible* spin-exchange coupling between the satellite transitions. Therefore, our description presented here holds for dynamic saturation of the central transition. On the other hand, if one dynamically saturates the outer high-frequency satellite, flip-flop transitions can take place between the central transitions, trying to "thermalize" them. This then leads to a reduction of the enhancement for the central transition as well as for the first satellite, since they share a common energy level, which could explain the observed discrepancy of the enhancement obtained between the saturation of the central line and of the outer satellite. Since the involved timescales for flip-flop transitions are unknown, it is difficult to estimate the magnitude of these effects. We believe, however, the higher value for W_2/W to be more reliable, since it stems from the dynamic saturation of the central transition. Hence, the weighted average for W_2/W is a lower estimate for the true ratio of W_2 and W.

To cross-check the results, we also performed an experiment with the so-called *gradual saturation sequence* which involves the application of all three pulse sequences as they are shown in Fig. 3. T_s is the duration of the saturation sequence. By I_s we denote the intensity of a line in case of gradual saturation while I_0 is the intensity of the line in the standard spin-echo sequence (including the heating sequence). The *gradual intensity enhancement* is then defined as I_s/I_0. In Fig. 5, we have plotted this enhancement for the central transition (top) and for the

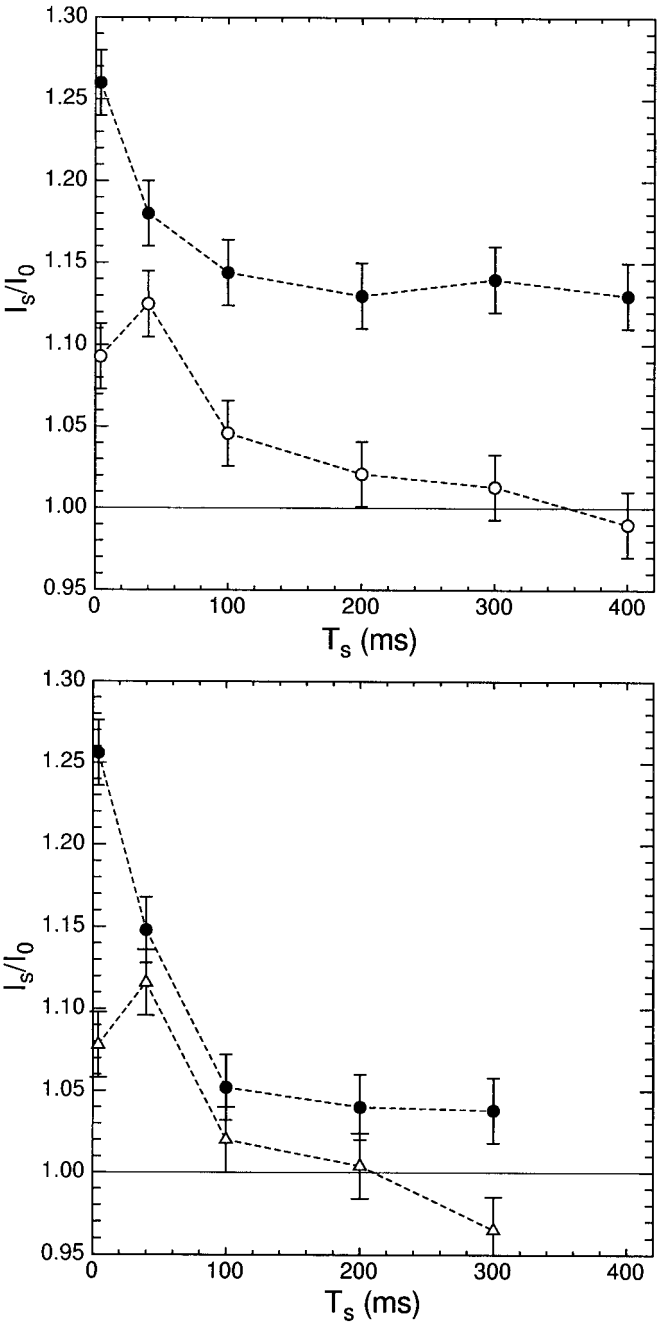

FIG. 5. Top: Gradual saturation of central transition. Full (open) bullets represent the intensity enhancement of the inner (outer) high-frequency satellites. Bottom: Gradual saturation of outer high-frequency satellite. Bullets (triangles) represent the intensity enhancement of the inner high-frequency satellite (central transition).

outer satellite (bottom) as a function of T_s. Bullets refer to inner satellites (top and bottom), open circles to outer satellites (top), and triangles (bottom) to the central transition.

For short T_s, the inner satellites (denoted by bullets) are strongly enhanced as expected, since in the case of an ideal $\pi/2$ pulse (adiabatic manipulation) at the central transition or outer satellite, respectively, I_s/I_0 should reach the value 1.5. Due to spin–lattice relaxation processes this value decays toward a limit which is 1 (for T_s reaching a value corresponding to dynamical saturation) in the case of pure magnetic relaxation and different from 1 in the case of mixed or pure quadrupolar relaxation.

The response of the outer satellite and the central transition enhancement is retarded, since spin–lattice relaxation processes need some time for "pumping" these transitions. This explains the enhancement maximum around $T_s = 40$ ms, before the enhancement starts to diminish toward 1 in the limit of dynamic saturation ($T_s \simeq 300 \cdots 350$ ms). In this limit, that is, for $T_s \to 1/\min(W, W_1, W_2)$, we have, according to Section 3 and Fig. 2, $I_s/I_0 \to E_m^{1/2}$. This is the results discussed above.

Due to technical reasons, we always applied the saturation pulses in pairs, i.e., one *C* pulse followed by a *D* pulse. This is the reason why in Fig. 5, for $T_s \to 0$, the open circles and triangles (outer satellite and central transition, respectively) do not approach 1, as one would expect, since the second pulse (*D* pulse) already pumps the higher transitions.

The experiment performed shows that the spin–lattice relaxation process contains a strong quadrupolar contribution which could not be detected otherwise so far. The discussion of the origin of this effect, which arises neither from phonons nor from defect motion of ions, as well as its temperature dependence will be given elsewhere (*19*).

5. SUMMARY

We have presented a pulse double-irradiation method which allows one to separate magnetic from quadrupolar contributions in the spin–lattice relaxation. The pulse sequence fully saturates one transition while another is observed. The clue is that the observed transition changes its intensity if and only if a $|\Delta m| = 2$ quadrupolar contribution is present; the change is monitored with respect to a standard spin-echo experiment. We calculated analytically this intensity change for spins $I = 1, \frac{3}{2}, \frac{5}{2}$, thus providing a quantitative analysis of the experimental results. Since the pulse sequence presented takes care of the absorbed radio-frequency power, no problems due to heating arise. The method is especially suited when only *one* NMR sensitive isotope is available. Different cross-checks were performed to prove the reliability of the results obtained.

The applicability of the method is demonstrated by a study of the plane oxygen ^{17}O ($I = \frac{5}{2}$) in the high-temperature superconductor $YBa_2Cu_4O_8$. We showed that the spin–lattice relaxation rate consists of magnetic as well as quadrupolar contributions.

APPENDIX: ANALYTICAL FORMULAE FOR INITIAL CONDITION VECTOR

A.1. Spin $I = 1$

$$\frac{\mathbf{N}(0)}{n_0} = \left[\frac{\mu}{\zeta}, -1\right], \quad \mu = 2W_2,\ \zeta = 2W + W_1 + 2W_2.$$

A.2. Spin $I = \frac{3}{2}$

(a) Dynamic Saturation of the Central Transition

$$\frac{\mathbf{N}(0)}{n_0} = \left[\frac{\mu}{\zeta}, -1, \frac{\mu}{\zeta}\right], \quad \mu = W_2,\ \zeta = 3W + W_1 + W_2.$$

(b) Dynamic Saturation of the Satellite

$$\frac{\mathbf{N}(0)}{n_0} = \left[-1, \frac{\mu_1}{\zeta}, \frac{\mu_2}{\zeta}\right],$$

$$\mu_1 = W_2(3W + W_1 + W_2)$$

$$\mu_2 = -W_2^2$$

$$\zeta = 12W^2 + 4WW_1 + 10WW_2 + 2W_1W_2 + W_2^2.$$

A.3. Spin $I = \frac{5}{2}$

(a) Dynamic Saturation of the Central Transition

$$\frac{\mathbf{N}(0)}{n_0} = \left[\frac{\mu_4}{\zeta_1}, \frac{\mu_5}{\zeta_1}, -1, \frac{\mu_5}{\zeta_1}, \frac{\mu_4}{\zeta_1}\right]$$

$$\mu_4 = -9W_2^2$$

$$\mu_5 = 45W_2(10W + 2W_1 + W_2)$$

$$\zeta_1 = 4000W^2 + 1000WW_1 + 40W_1^2 + 1100WW_2 + 160W_1W_2 + 45W_2^2.$$

(b) Dynamic Saturation of the Inner Satellite

$$\frac{\mathbf{N}(0)}{n_0} = \left[\frac{\mu_6}{\zeta_2}, -1, \frac{\mu_6}{\zeta_2}, \frac{\mu_7}{\zeta_2}, \frac{\mu_8}{\zeta_2}\right]$$

$$\mu_6 = W_2(8000W^3 + 2000W^2W_1 + 80WW_1^2 + 3800W^2W_2 + 720WW_1W_2 + 16W_1^2W_2 + 440WW_2^2 + 46W_1W_2^2 + 9W_2^3)$$

$$\mu_7 = -9W_2^2(10W + 2W_1 + W_2)^2$$

$$\mu_8 = 9W_2^3(10W + 2W_1 + W_2)$$

$$\zeta_2 = 80{,}000W^4 + 36{,}000W^3W_1 + 4800W^2W_1^2 + 160WW_1^3 + 8200W^2W_2^2 + 46{,}000W^3W_2 + 16{,}800W^2W_1W_2 + 1680WW_1^2W_2$$

$$+ 32W_1^3W_2 + 2060WW_1W_2^2 + 108W_1^2W_2^2$$
$$+ 530WW_2^3 + 64W_1W_2^3 + 9W_2^4.$$

(c) Dynamic Saturation of the Outer Satellite

$$\frac{\mathbf{N}(0)}{n_0} = \left[-1, \frac{\mu_9}{\zeta_3}, \frac{\mu_{10}}{\zeta_3}, \frac{\mu_{11}}{\zeta_3}, \frac{\mu_{12}}{\zeta_3} \right]$$

$$\mu_9 = W_2(8000W^3 + 2000W^2W_1 + 80WW_1^2 + 3800W^2W_2 + 720WW_1W_2 + 16W_1^2W_2 + 440WW_2^2 + 46W_1W_2^2 + 9W_2^3)$$

$$\mu_{10} = -W_2^2(800W^2 + 200WW_1 + 8W_1^2 + 220WW_2 + 32W_1W_2 + 9W_2^2)$$

$$\mu_{11} = 9W_2^3(10W + 2W_1 + W_2)$$

$$\mu_{12} = -9W_2^4$$

$$\zeta_3 = 128{,}000W^4 + 38{,}400W^3W_1 + 2880W^2W_1^2 + 64WW_1^3 + 83{,}200W^3W_2 + 20{,}160W^2W_1W_2 + 1056WW_1^2W_2 + \tfrac{64}{5}W_1^3W_2 + 16{,}240W^2W_2^2 + 2744WW_1W_2^2 + \tfrac{336}{5}W_1^2W_2^2 + 980WW_2^3 + \tfrac{392}{5}W_1W_2^3 + 9W_2^4.$$

ACKNOWLEDGMENT

The partial support of this work by the Swiss National Science Foundation is gratefully acknowledged.

REFERENCES

1. E. R. Andrew and D. P. Tunstall, *Proc. Phys. Soc.* **78,** 1 (1961).
2. D. P. Tewari and G. S. Verma, *Phys. Rev.* **129,** 1975 (1963).
3. A. Narath, *Phys. Rev.* **162,** 320 (1967).
4. M. I. Gordon and M. J. R. Hoch, *J. Phys. C: Solid State Phys.* **11,** 783 (1978).
5. A. F. McDowell, *J. Magn. Reson. A* **113,** 242 (1995).
6. A. C. Daniel and W. G. Moulton, *J. Chem. Phys.* **41,** 1833 (1964).
7. N. E. Ainbinder and I. G. Shaposhnikov, "Advances in Nuclear Quadrupole Resonance" (J. A. S. Smith, Ed.), Heyden & Son, London (1978).
8. J. Chepin and J. H. Ross, Jr., *J. Phys.: Condens. Matter* **3,** 8103 (1991).
9. I. Watanabe, *J. Phys. Soc. Jpn.* **63,** 1560 (1994).
10. D. E. MacLaughlin, J. D. Williamson, and J. Butterworth, *Phys. Rev. B* **4,** 60 (1971).
11. T. Rega, *J. Phys.: Condens. Matter* **3,** 1871 (1991).
12. A. Suter, M. Mali, J. Roos, and D. Brinkmann, *J. Phys.: Condens. Matter* **10,** 5977 (1998).
13. R. V. Pound, *Phys. Rev.* **79,** 685 (1950).
14. A. Abragam, "The Principles of Nuclear Magnetism," Clarendon, Oxford (1961).
15. C. P. Slichter, "Principles of Magnetic Resonance," Springer-Verlag, New York/Berlin/Heidelberg (1992).
16. D. Brinkmann, M. Mali, J. Roos, R. Messer, and H. Birli, *Phys. Rev. B* **26,** 4810 (1982).
17. M. Takigawa, J. L. Smith, and W. L. Hults, *Phys. Rev. B* **44,** 7764 (1991).
18. M. Horvatić, *J. Phys.: Condens. Matter* **4,** 5811 (1992).
19. A. Suter, M. Mali, J. Roos, and D. Brinkmann, submitted for publication.
20. H. Zimmermann, Ph.D. thesis, Universität Zürich (1991).
21. I. Mangelschots, M. Mali, J. Roos, D. Brinkmann, S. Rusiecki, J. Karpinski, and E. Kaldis, *Physica C* **194,** 277 (1992).
22. F. Raffa, T. Ohno, M. Mali, J. Roos, D. Brinkmann, K. Conder, and M. Eremin, *Phys. Rev. Lett.* **81,** 5912 (1998).
23. A. Suter, M. Mali, J. Roos, D. Brinkmann, J. Karpinski, and E. Kaldis, *Phys. Rev. B* **56,** 5542 (1997).